Maximal and total skew information of three-qubit system obtained using nonlinear interaction models*

Sun Hong-Gui(孙红贵)[a)†], Zhang Li-Hua(章礼华)[b)],
Liu Wan-Fang(刘万芳)[b)], and Li Chun-Jie(李春杰)[c)]

[a)] *Mechanical and Electrical Engineering College, Jiaxing University, Jiaxing* 314001, *China*
[b)] *School of Physics and Electric Engineering, Anqing Teachers College, Anqing* 246011, *China*
[c)] *College of Physics, Changchun Normal University, Changchun* 130032, *China*

(Received 8 November 2010; revised manuscript received 5 September 2011)

Both the maximal and the total skew information have been studied. For a three-qubit system implemented in three nonlinear interaction models, we give the exact state vector at any time t. Based on this, we give the maximal and the total skew information. It is found that they have the same form and their evolution periods are dependent on the energy difference between the ground state and the second excited state in these models. The maximal skew information is always in the (S_x, S_y) plane. We give the condition for the occurrence of $|\mathrm{GHZ}\rangle_{S_y}$, in which they can reach the extreme values of 9/4 and 15/4, respectively. In three different decoherence channels, two kinds of information and the concurrence are calculated. We find that the phenomenon of the concurrence of sudden death occurs, but the above two kinds of information do not die suddenly. In the phase-damping channel, the two kinds of information will not be lost completely.

Keywords: maximal and total Wigner–Yanase skew information, nonlinear interaction models, three-qubit system, three decoherence channels

PACS: 03.65.–w, 03.67.–a, 05.45.–a **DOI:** 10.1088/1674-1056/21/1/010301

1. Introduction

It is well known that spin squeezing is connected with the minimum spin fluctuation in the plane that is perpendicular to the mean spin direction.[1−3] To generate spin squeezing and spin squeezed states, Kitagawa and Ueda first introduced the one-axis twisting and the two-axis countertwisting models.[1] Subsequently, the one-axis twisting model has been studied widely.[4−8] It was shown that an external field in the one-axis twisting model as well as in the two-axis countertwisting model can improve the spin squeezing and the entanglement.[9,10] Possible realizations of the one-axis twisting Hamiltonian have been studied in a two-component Bose–Einstein condensate[11−16] and an atomic ensemble system in the dispersive regime. Sørensen *et al.* also proposed that spin squeezing can be used as a measure of many-particle quantum entanglement.[11] In the above models, only the one-axis twisting model can be solved analytically within the Heisenberg picture. However, for a system with a few spins[17−22] the exact solutions for the state vectors of the models are possible at any time t.

The Wigner–Yanase skew information corresponds to the fluctuation of a pure state.[23] It is essentially a particular kind of quantum Fisher information[24−26] and is closely connected to the Heisenberg uncertainty principle.[27,28] It has been shown that it can be used to detect entanglement.[29] However, the study of the Wigner–Yanase skew information in a spin system is still lacking. Based on the concept of the Wigner–Yanase skew information, the maximal Wigner–Yanase skew information (MSI) and the total Wigner–Yanase skew information (TSI) are introduced. For the two-qubit pure states, they are equivalent to the spin squeezing and concurrence that is a measure of the degree of the two-qubit entanglement.[30−33] In this paper, for a three-qubit system, in terms of the eigenstates of S_z, we first present the states generated via the one-axis twisting model with an external field, the two-axis counter-

*Project supported by the College Young Talents Foundation of Anhui Province, China (Grant No. 2010SQRL107), the Natural Science Foundation of the Education Department of Anhui Province, China (Grant No. KJ2008B83ZC) and the Natural Science Foundation of Anhui Province, China (Grant No. KJ2011Z234).

†Corresponding author. E-mail: hongguisun@gmail.com

© 2012 Chinese Physical Society and IOP Publishing Ltd

twisting model with an external field, and a mixture of the two models. Further, we will study the MSI and the TSI of the states and find the nonlinear interactions among the elementary spins that are important ingredients for good MSI and TSI. Moreover, we can show that one of them possesses the same form in the three models. We give a requirement of the external field for the occurrence of $|\mathrm{GHZ}\rangle_{S_y}$ state. On the quantum resource, the effects of the environment surrounding the quantum system are very important, so naturally we should consider the decay of the quantum state. In order to examine the capacity of the skew information to overcome decoherence, we calculate the MSI and the TSI in three different decoherence channels within the Heisenberg picture.

This paper is organized as follows. In Section 2, we study the relation between the MSI, the TSI, and the linear entropy in symmetric pure states. In Section 3, we consider three nonlinear models for a three-qubit system, then present the explicit expressions for the state vectors at any time t and study the MSI and the TSI. In Section 4, we further study the MSI, the TSI, and the concurrence of these models with three qubits in three different decoherence channels. Finally, a conclusion is given in Section 5.

2. Theoretical model

Let us first review the concept of the Wigner–Yanase skew information. In order to further study the measurement theory from an information-theory point of view, Wigner and Yanase introduced a quantity[23] called the Wigner–Yanase skew information (SI), which is the amount of information of the observables not commuting with A. In terms of the density matrix ρ and the operator A, it is defined as[23]

$$I(\rho, A) = -\frac{1}{2}\,\mathrm{Tr}[\rho^{1/2}, A]^2. \tag{1}$$

From Eq. (1), we know that $I(\rho, A)$ may be interpreted as the degree of non-commutativity between ρ and A.[34] Note that the SI can be rewritten as

$$I(\rho, A) = \mathrm{Tr}\,\rho A^2 - \mathrm{Tr}\,\rho^{1/2} A \rho^{1/2} A. \tag{2}$$

In particular, if the pure state of a system is considered, then this state can be described by $|\psi\rangle$. The corresponding density matrix ρ has the property $\rho^k = \rho$. So the SI of the state has the following form:

$$I(\rho, A) = \langle\psi|A^2|\psi\rangle - \langle\psi|A|\psi\rangle^2. \tag{3}$$

It is actually the fluctuation of operator A. A collection of N spin-$\frac{1}{2}$ particles are represented by the collective operators

$$S_\mu = \sum_{i=1}^{N} S_{i,\mu},\ \mu \in \{x, y, z\}, \tag{4}$$

where $S_{i,\mu}$ are the spin operators for the i-th qubit. The cyclic commutation relations are satisfied

$$[S_{i,\mu}, S_{i,\nu}] = \mathrm{i}\,\epsilon_{\mu\nu\gamma} S_{i,\gamma}, \tag{5}$$

$$[S_\mu, S_\nu] = \mathrm{i}\,\epsilon_{\mu\nu\gamma} S_\gamma, \quad \mu, \nu, \gamma \in \{x, y, z\}, \tag{6}$$

where $\epsilon_{\mu\nu\gamma}$ is the Levi–Civita symbol. For the pure states, as the SI equals the spin fluctuation the MSI is actually the maximal spin fluctuation, and we use I_m to denote this quantity. If the mean spin direction $\boldsymbol{n}_1$ is along the z axis, and its collective angular momentum operators satisfy the condition $\langle[S_z, S_x]_+\rangle = \langle[S_z, S_y]_+\rangle = 0$, then the maximal spin fluctuation has the following form:[8]

$$\max(\Delta S_{\boldsymbol{n}})^2 = \max(\Delta S_z^2, \max \Delta S^2(x, y)), \tag{7}$$

where $S_{\boldsymbol{n}}$ is defined as

$$S_{\boldsymbol{n}} = \sin\Theta\cos\Phi S_x + \sin\Theta\sin\Phi S_y + \cos\Theta S_z,$$

and $\max \Delta S^2(x, y)$ is the maximum fluctuation in the (S_x, S_y) spin plane.[8] We can use the method in Refs. [4], [35], and [36] to obtain

$$\max \Delta S^2(x, y) = \frac{1}{2}(S^2 + S - \langle S_z^2\rangle + |\langle S_+^2\rangle|). \tag{8}$$

Fortunately, in the states generated by both the one-axis and the two-axis models, the mean spin direction $\boldsymbol{n}_1$ is along the z axis, and the condition $\langle[S_z, S_x]_+\rangle = \langle[S_z, S_y]_+\rangle = 0$ can be satisfied.

Based on the SI, we can define a quantity that is the sum of the SI in the x, y, and z directions and will be called the total skew information. For convenience, we denote it as

$$I_\mathrm{sum} = \sum_\mu \Delta S_\mu^2,\ \mu \in \{x, y, z\}. \tag{9}$$

On the other hand, the linear entropy is defined as[37,38]

$$E_\mathrm{L} = 1 - \mathrm{Tr}(\rho_i^2), \tag{10}$$

where ρ_i is the reduced matrix of the i-th particle. For the states belonging to the subspace with the maximal spin angular momentum $S = N/2$, there is a clear relation between the linear entropy and the expectation values of S_μ

$$E_\mathrm{L} = \frac{1}{2}\left[1 - \frac{4}{N^2}(\langle S_x\rangle^2 + \langle S_y\rangle^2 + \langle S_z\rangle^2)\right]. \tag{11}$$

Then we can obtain the relation between the linear entropy and the TSI

$$I_{\rm sum} = \frac{N}{2} + \frac{N^2}{2} E_{\rm L}. \tag{12}$$

If the condition $\langle S_x \rangle = \langle S_y \rangle = 0$ can be satisfied in Eq. (11), for example, in the one-axis and the two-axis models,[7−16] then the linear entropy and $I_{\rm sum}$ depend on $\langle S_z \rangle^2$ as follows:

$$E_{\rm L} = \frac{1}{2}[1 - \frac{4}{N^2}\langle S_z \rangle^2], \tag{13}$$

$$I_{\rm sum} = S(S+1) - \langle S_z \rangle^2. \tag{14}$$

Under the above restrictive condition, $\langle S_z \rangle^2$ is an essential ingredient of the linear entropy and the TSI. In the following section, we focus on the calculation of $\langle S_z \rangle$, $\langle S_z^2 \rangle$, and $|\langle S_+^2 \rangle|$.

3. Maximal and total skew information of nonlinear interaction models for three-qubit system

Now we study the MSI and the TSI of the three-qubit pure states dynamically generated from $|111\rangle$ via the following three nonlinear interaction Hamiltonian models, which do not change the parity of the initial state. Quantum mechanics indicates that if the initial state of a system can be expressed as a linear combination of the eigenstates of the Hamiltonian that is independent of time, i.e., $\psi(0) = \sum_n c_n \phi_n$, then the final state can be given by $\psi(t) = \sum_n {\rm e}^{-{\rm i}E_n t} c_n \phi_n$, where E_n is the eigenvalue corresponding to eigenstate ϕ_n. Here we let $\hbar = 1$. We can then study the information included in the final state $\psi(t)$. For our problem the first thing we need to do is find the eigenvalues and the eigenstates of these nonlinear interaction Hamiltonian models. For the case of a small number of particles, the task is easy; here we only consider the three-qubit case. Our central task is to calculate the expectation values of $\langle S_z \rangle$, $\langle S_z^2 \rangle$, and $|\langle S_+^2 \rangle|$ at any time t.

3.1. One-axis twisting model with an external field

The first model is the one-axis twisting model with an external field. The corresponding Hamiltonian can be described by[5,9,15,16]

$$H = 2\chi_1 S_x^2 + \Omega S_z, \tag{15}$$

where Ω (> 0) can be controlled by the strength of the external field, and χ_1 describes the nonlinear interaction strength of the quantum correlations among the elementary spins.[1] Several studies have identified that the nonlinear interaction $2\chi_1 S_x^2$ can be naturally found in a trapped Bose condensate.[11,39,40] In practice, the Hamiltonian given by Eq. (15) can be applied to a trapped spinor Bose condensate. If the initial state is $|111\rangle$, we find that only two eigenstates $\phi_\pm$ and two energies $E_\pm$ are useful to our task by solving the eigenvalue equation of the Hamiltonian. State ϕ_+ is the second excited state with energy E_+, state ϕ_- is the ground state with energy E_-. Their exact expressions are

$$\phi_\pm = \frac{1}{A_\pm} \begin{pmatrix} 0 \\ \dfrac{(\Omega + \chi_1 \pm \sqrt{\Omega^2 + 2\Omega\chi_1 + 4\chi_1^2})}{\sqrt{3}\chi_1} \\ 0 \\ 1 \end{pmatrix}, \tag{16}$$

$$E_\pm = -\frac{\Omega}{2} + \frac{5\chi_1}{2} \pm \sqrt{\Omega^2 + 2\Omega\chi_1 + 4\chi_1^2}, \tag{17}$$

where $A_\pm$ are the normalization factors given by

$$A_\pm = \sqrt{3}\chi_1 \{2[(\Omega + \chi_1)^2 + 3\chi_1^2 + (\Omega + \chi_1)\sqrt{\Omega^2 + 2\Omega\chi_1 + 4\chi_1^2}]\}^{-1/2}. \tag{18}$$

If we set $W = \Omega + \chi_1$ and $\chi = \sqrt{3}\chi_1$, then the eigenstates and the eigenvalues can be reduced to

$$\phi_\pm = \frac{1}{A_\pm} \begin{pmatrix} 0 \\ \dfrac{(W \pm \sqrt{W^2 + \chi^2})}{\chi} \\ 0 \\ 1 \end{pmatrix}, \tag{19}$$

$$A_\pm = \chi[2(W^2 + \chi^2 \pm W\sqrt{W^2 + \chi^2})]^{-1/2}, \tag{20}$$

$$E_\pm = -\frac{\Omega}{2} + \frac{5\chi_1}{2} \pm \sqrt{W^2 + \chi^2}. \tag{21}$$

Under the initial condition $c_+\phi_+ + c_-\phi_- \equiv |111\rangle$, we can obtain coefficients $c_\pm$ and the final state vector as

$$c_\pm = \frac{\sqrt{W^2 + \chi^2} \mp W}{2\sqrt{W^2 + \chi^2}}, \tag{22}$$

$$\psi(t) = \begin{pmatrix} 0 & a(t) & 0 & b(t) \end{pmatrix}^{\rm T}, \tag{23}$$

$$a(t) = \chi \frac{{\rm e}^{-{\rm i}E_+ t} - {\rm e}^{-{\rm i}E_- t}}{2\sqrt{W^2 + \chi^2}}, \tag{24}$$

$$b(t) = \frac{({\rm e}^{-{\rm i}E_+ t} + {\rm e}^{-{\rm i}E_- t})}{2} - \frac{W({\rm e}^{-{\rm i}E_+ t} - {\rm e}^{-{\rm i}E_- t})}{2\sqrt{W^2 + \chi^2}}. \tag{25}$$

In order to obtain the MSI and the TSI, we must obtain the expectation values of $\langle S_z\rangle$, $\langle S_z^2\rangle$, and $|\langle S_+^2\rangle|$. Based on the state vector $\psi(t)$, by a straightforward calculation, we can give their exact expressions as

$$\langle S_z\rangle = \frac{-[3W^2+\chi^2+2\chi^2\cos(2\sqrt{W^2+\chi^2}t)]}{2(W^2+\chi^2)}, \quad (26)$$

$$\langle S_z^2\rangle = \frac{[9W^2+5\chi^2+4\chi^2\cos(2\sqrt{W^2+\chi^2}t)]}{4(W^2+\chi^2)}, \quad (27)$$

$$|\langle S_+^2\rangle| = \{2W^2[1-\cos(2\sqrt{W^2+\chi^2}t)] + \chi^2\sin^2(2\sqrt{W^2+\chi^2}t)\}^{1/2}\frac{\sqrt{3}\chi}{(W^2+\chi^2)}. \quad (28)$$

These quantities are periodic functions with a time scale ΔE, where $\Delta E = E_+ - E_- = 2\sqrt{W^2+\chi^2}$ is the energy difference between the second excited state and the ground state. Then the MSI and the TSI have the extreme values synchronously. We find that the MSI is always in the (S_x, S_y) plane when an arbitrary external field is present. For comparison, we present ΔS_z^2 and $\max \Delta S^2(x,y)$ in Figs. 1(a) and 1(b). This conclusion is still valid for the other two models, as shown in Figs. 2 and 3. When no external field is involved, the MSI and the TSI have the extreme values 9/4 and 15/4 at time $t_{\rm m} = \pi/\Delta E$, respectively, as shown in Figs. 1(a) and 1(c). We can explain this by investigating state $\psi(t_{\rm m})$. By a simple calculation, we observe that $\psi(t_{\rm m})$ has a simple form, which can be rewritten as the superposition of eigenstates $|\frac{3}{2}, \pm\frac{3}{2}\rangle_{s_y}$ of S_y with eigenvalues $\pm\frac{3}{2}$

$$\psi(t_{\rm m}) = \begin{pmatrix} 0 & \frac{\sqrt{3}}{2} & 0 & -\frac{1}{2}\end{pmatrix}^{\rm T} = \frac{1}{\sqrt{2}}\left(\left|\frac{3}{2},\frac{3}{2}\right\rangle_{s_y} - \left|\frac{3}{2},-\frac{3}{2}\right\rangle_{s_y}\right), \quad (29)$$

where

$$\left|\frac{3}{2},\frac{3}{2}\right\rangle_{s_y} = \begin{pmatrix} \frac{\sqrt{2}}{4}\,{\rm i} & \sqrt{\frac{3}{8}} & -\sqrt{\frac{3}{8}}\,{\rm i} & -\frac{\sqrt{2}}{4}\end{pmatrix}^{\rm T},$$
$$\left|\frac{3}{2},-\frac{3}{2}\right\rangle_{s_y} = \begin{pmatrix} \frac{\sqrt{2}}{4}\,{\rm i} & -\sqrt{\frac{3}{8}} & -\sqrt{\frac{3}{8}}\,{\rm i} & \frac{\sqrt{2}}{4}\end{pmatrix}^{\rm T}. \quad (30)$$

As $\langle S_\mu\rangle = 0$ and $\mu \in \{x, y, z\}$, it is obvious that the state is $|{\rm GHZ}\rangle_{S_y}$ with the maximal fluctuation $I_{\rm m} = \Delta S_y^2 = 9/4$ for the extreme MSI and $I_{\rm sum} = 15/4$ for the extreme TSI. It is worth noting that at time $t_{\rm m}$, the linear entropy equals 0.5, but the concurrence is 0. This implies that the extreme MSI and TSI do not correspond to the maximal concurrence (Figs. 1(c) and 1(d)), which is different from the two-qubit case. With the increase of Ω, the extreme values of the MSI and the TSI decrease in the presence of external fields. In fact, for the case of $\Omega \gg \chi_1$, the nonlinear term $2\chi_1 S_x^2$ can be treated as a perturbation, then the states of the system and the expectation values $\langle\hat{F}\rangle$ do not deviate too far away from their initial values. This illustrates that the quantum correlation among individual qubits is an essential ingredient to obtain good MSI and good TSI.

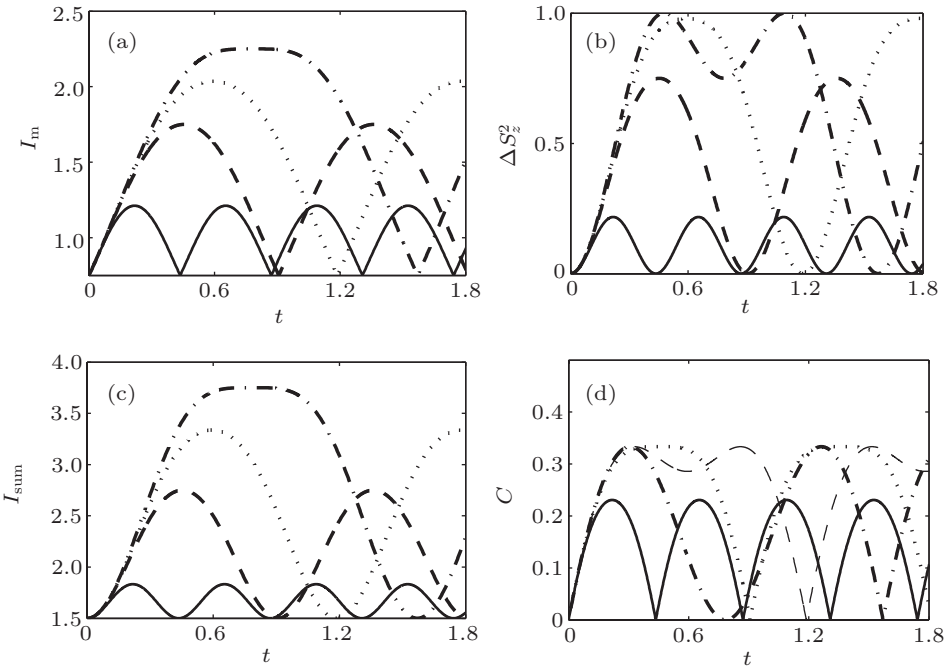


Fig. 1. (a) $I_{\rm m}$, (b) ΔS_z^2, (C) $I_{\rm sum}$, and (d) C versus t with $\chi_1 = 1$. Parameter Ω takes 0, 1, 2, and 6 for dot-dashed, dotted, dashed, and solid lines, respectively.

3.2. Two-axis countertwisting model with an external field

Consider the two-axis countertwisting model with an external field. The Hamiltonian can be put as[9,15]

$$H = \frac{\chi_2}{2\,\mathrm{i}}(S_+^2 - S_-^2) + \Omega S_z. \tag{31}$$

It is actually the LMG model. The LMG model, originally introduced in nuclear physics, has been widely studied in other fields including statistical mechanics of quantum spin system,[41] the Bose–Einstein condensates,[42] and magnetic molecules such as Mn_{12} acetate.[43] The exact diagonalization of the Hamiltonian provides two available eigenstates and two eigenvalues

$$\phi_\pm = \frac{1}{A_\pm}\begin{pmatrix} 0 \\ \dfrac{-\mathrm{i}(W \pm \sqrt{W^2+\chi^2})}{\chi} \\ 0 \\ 1 \end{pmatrix}, \tag{32}$$

$$A_\pm = \chi[2(W^2+\chi^2 \pm W\sqrt{W^2+\chi^2})]^{-1/2}, \tag{33}$$

$$E_\pm = -\frac{W}{2} \pm \sqrt{W^2+\chi^2}, \tag{34}$$

where $W = \Omega$, $\chi = \sqrt{3}\chi_2$, and $A_\pm$ are the normalization factors. The second excited state ϕ_+ and the ground state ϕ_- correspond to E_+ and E_-, respectively. The expansion coefficients and the final state vector are obtained as

$$c_\pm = \frac{\sqrt{W^2+\chi^2} \mp W}{2\sqrt{W^2+\chi^2}}, \tag{35}$$

$$\psi(t) = \begin{pmatrix} 0 & a(t) & 0 & b(t) \end{pmatrix}^{\mathrm{T}}, \tag{36}$$

$$a(t) = \mathrm{i}\,\chi\frac{\mathrm{e}^{-\mathrm{i}\,E_+ t} - \mathrm{e}^{-\mathrm{i}\,E_- t}}{2\sqrt{W^2+\chi^2}}, \tag{37}$$

$$b(t) = \frac{(\mathrm{e}^{-\mathrm{i}\,E_+ t} + \mathrm{e}^{-\mathrm{i}\,E_- t})}{2} - \frac{W(\mathrm{e}^{-\mathrm{i}\,E_+ t} - \mathrm{e}^{-\mathrm{i}\,E_- t})}{2\sqrt{W^2+\chi^2}}. \tag{38}$$

The expectation value $\langle S_z\rangle$ at any time t is given by

$$\langle S_z\rangle = \frac{-[3W^2+\chi^2+2\chi^2\cos(2\sqrt{W^2+\chi^2}t)]}{2(W^2+\chi^2)}, \tag{39}$$

$$\langle S_z^2\rangle = \frac{[9W^2+5\chi^2+4\chi^2\cos(2\sqrt{W^2+\chi^2}t)]}{4(W^2+\chi^2)}, \tag{40}$$

$$|\langle S_+^2\rangle| = \{2W^2[1-\cos(2\sqrt{W^2+\chi^2}t)] + \chi^2\sin^2(2\sqrt{W^2+\chi^2}t)\}^{1/2}\frac{\sqrt{3}\chi}{(W^2+\chi^2)}. \tag{41}$$

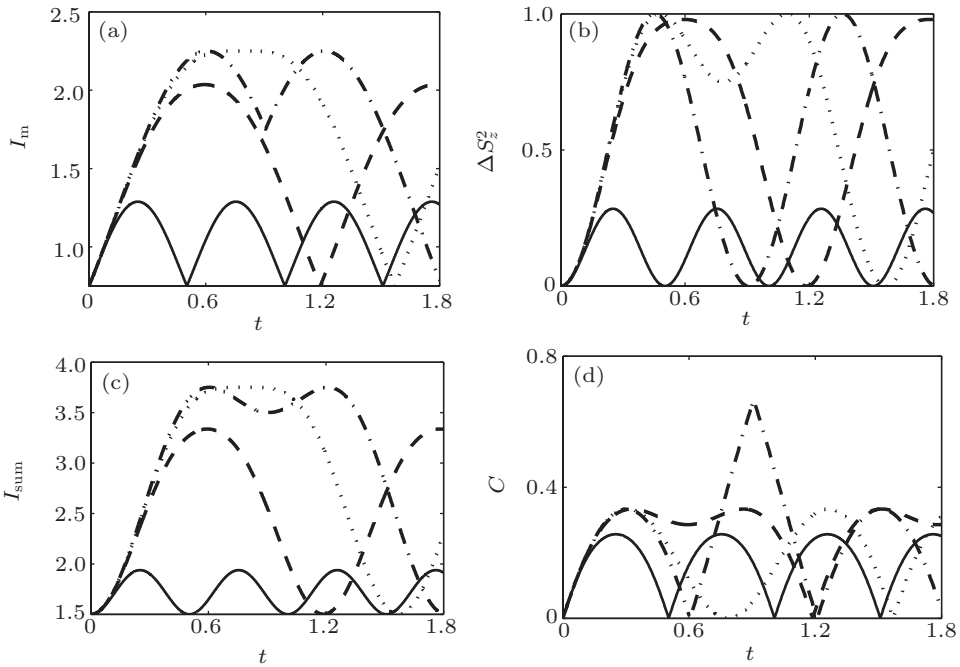


Fig. 2. (a) I_{m}, (b) ΔS_z^2, (c) I_{sum}, and (d) C versus t with $\chi_2 = 1$. Parameter Ω takes 0, 1, 2, and 6 for dot-dashed, dotted, dashed, and solid lines, respectively.

Though the result is the same as that of the first model, there are some differences for the time evolution of the MSI and the TSI. We present $I_{\rm m}$ and $I_{\rm sum}$ in Figs. 2(a) and 2(c), respectively. We observe that for the case with $\Omega = 0$, their extreme values occur at time $t^*_{\rm m} = 2\pi/(3\Delta E)$ not at $t_{\rm m}$. The state vectors at the two time points are

$$\psi(t^*_{\rm m}) = \begin{pmatrix} 0 \\ \frac{\sqrt{3}}{2} \\ 0 \\ -\frac{1}{2} \end{pmatrix}, \quad \psi(t_{\rm m}) = \begin{pmatrix} 0 \\ 1 \\ 0 \\ 0 \end{pmatrix}. \tag{42}$$

Here $\psi(t^*_{\rm m})$ is the $|{\rm GHZ}\rangle_{S_y}$ with the extreme $I_{\rm m} = 9/4$, the extreme $I_{\rm sum} = 15/4$, and the minimum concurrence $C = 0$. The $\psi(t_{\rm m})$ is the eigenstate of operator S_z with $I_{\rm m} = 7/4$ and $I_{\rm sum} = 14/4$. By using the formula in Ref. [44], we can demonstrate that the concurrence equals $2/3$ at $t_{\rm m}$. For comparison, we present the time evolution of the concurrence in Fig. 2(d). If W is in the region of $0 \leq W \leq \chi/\sqrt{3}$, the extreme values of $I_{\rm m}$ and $I_{\rm sum}$ do not change. There is a time region $t^*_{\rm m} \leq t \leq t_{\rm m}$, at which the extreme values of the MSI and the TSI will occur. However, the maximal value of C varies with W. With the increase of Ω, the extreme values of the MSI and the TSI decrease when $W > \chi/\sqrt{3}$. For the case of $\Omega \gg \chi_1$, the nonlinear term $2\chi_1 S_x^2$ can also be treated as a perturbation.

3.3. Mixed model with an external field

Now, we consider a general model, which is the mixed model of the one-axis twisting and the two-axis countertwisting models with an external field. The Hamiltonian reads

$$H = \chi_1 S_x^2 + \frac{\chi_2}{2\,{\rm i}}(S_+^2 - S_-^2) + \Omega S_z. \tag{43}$$

The two eigenstates are

$$\phi_\pm = \frac{1}{A_\pm} \begin{pmatrix} 0 \\ \frac{\sqrt{3}(\chi_1 - {\rm i}\,\chi_2)(W \pm \sqrt{W^2+\chi^2})}{\chi^2} \\ 0 \\ 1 \end{pmatrix}, \tag{44}$$

with the normalization factors

$$A_\pm = \chi[2(W^2 + \chi^2 \pm W\sqrt{W^2+\chi^2})]^{-1/2}, \tag{45}$$

where $W = \Omega + \chi_1$ and $\chi^2 = 3(\chi_1^2 + \chi_2^2)$. The two corresponding eigenvalues are

$$E_\pm = -\frac{\Omega}{2} + \frac{5\chi_1}{2} \pm \sqrt{W^2+\chi^2}. \tag{46}$$

We obtain the expansion coefficients and the final state under the initial condition $\psi(0) = |111\rangle$ as

$$c_\pm = \frac{\sqrt{W^2+\chi^2} \mp W}{2\sqrt{W^2+\chi^2}}, \tag{47}$$

$$\psi(t) = \begin{pmatrix} 0 & a(t) & 0 & b(t) \end{pmatrix}^{\rm T}, \tag{48}$$

$$a(t) = \frac{\sqrt{3}(\chi_1 - {\rm i}\,\chi_2)({\rm e}^{-{\rm i}\,E_+ t} - {\rm e}^{-{\rm i}\,E_- t})}{2\sqrt{W^2+\chi^2}}, \tag{49}$$

$$b(t) = \frac{({\rm e}^{-{\rm i}\,E_+ t} + {\rm e}^{-{\rm i}\,E_- t})}{2} - \frac{W({\rm e}^{-{\rm i}\,E_+ t} - {\rm e}^{-{\rm i}\,E_- t})}{2\sqrt{W^2+\chi^2}}, \tag{50}$$

and the expectation values are

$$\langle S_z \rangle = \frac{-[3W^2 + \chi^2 + 2\chi^2\cos(2\sqrt{W^2+\chi^2}t)]}{2(W^2+\chi^2)}, \tag{51}$$

$$\langle S_z^2 \rangle = \frac{[9W^2 + 5\chi^2 + 4\chi^2\cos(2\sqrt{W^2+\chi^2}t)]}{4(W^2+\chi^2)}, \tag{52}$$

$$|\langle S_+^2 \rangle| = \{2W^2[1 - \cos(2\sqrt{W^2+\chi^2}t)] + \chi^2\sin^2(2\sqrt{W^2+\chi^2}t)\}^{1/2}\frac{\sqrt{3}\chi}{(W^2+\chi^2)}. \tag{53}$$

We can see that $\langle S_z \rangle$, $\langle S_z^2 \rangle$, and $|\langle S_+^2 \rangle|$ have the same forms as those of the above two models. The W and χ possess different definitions for different models. In this model, if $\chi_1 = 0$ or $\chi_2 = 0$, it can be reduced to the second or the first model. So, we only discuss a general case, in which $\chi_1 \neq 0$ and $\chi_2 \neq 0$. As an example, we set $\chi_1 = \chi_2 = 1$. We present the corresponding $I_{\rm m}$, $I_{\rm sum}$, ΔS_z^2, and C in Fig. 3. We find that the evolutions of the four quantities are similar to those of the second model. If $0 \leq \Omega \leq \sqrt{\chi_1^2+\chi_2^2} - \chi_1$, the MSI and the TSI have extreme values $9/4$ and $15/4$, respectively. For the cases of $\Omega = 0$ and $\Omega = \sqrt{\chi_1^2+\chi_2^2} - \chi_1$, they occur at time $\arccos(-\frac{3}{4})/\Delta E$ and $t_{\rm m}$, respectively. For a general case of $0 < \Omega < \sqrt{\chi_1^2+\chi_2^2} - \chi_1$, they occur in the region of $\arccos(-\frac{3}{4})/\Delta E \leq t \leq t_{\rm m}$.

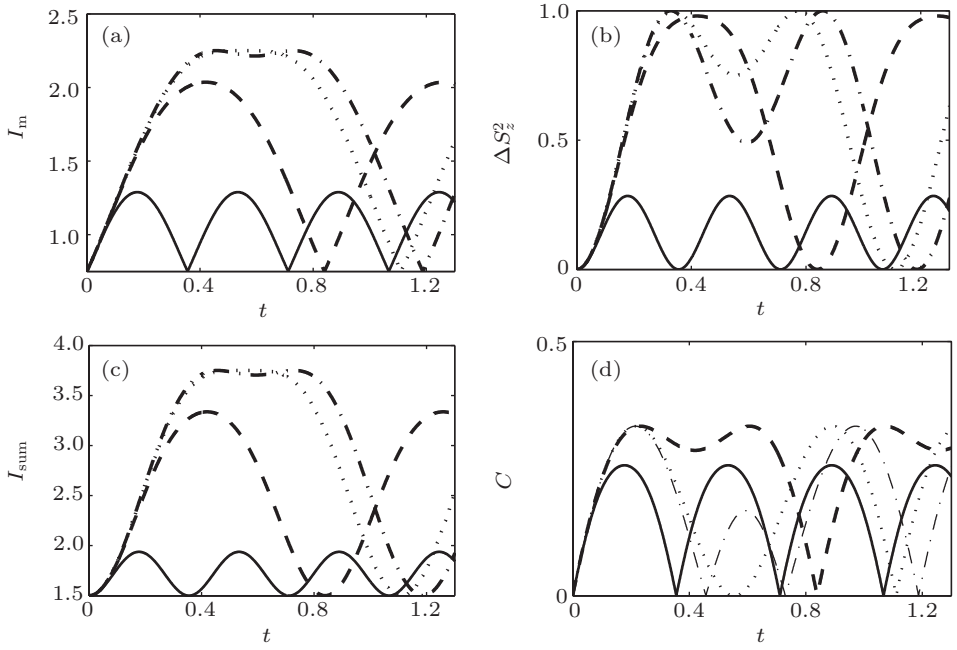


Fig. 3. (a) $I_{\rm m}$, (b) ΔS_z^2, (c) $I_{\rm sum}$, and (d) C versus t with $\chi_1 = \chi_2 = 1$. Parameter Ω takes 0, $\sqrt{2}-1$, $2\sqrt{2}-1$, and $6\sqrt{2}-1$ for dot-dashed, dotted, dashed, and solid lines, respectively.

4. Maximal and total skew information and concurrence under decoherence

4.1. Three decoherence channels

It is well known that quantum decoherence is an inevitable issue in quantum information processing. The typical decoherence channels include the amplitude-damping channel (ADC), the phase-damping channel (PDC), and the depolarizing channel (DPC). There are two equivalent methods for the study of the effects of decoherence. One method takes into account the decoherence mechanism in the quantum states, and the operators do not change. In general, the quantum states become mixed. The other considers the decoherence mechanism in the operators, and its advantage is that the quantum states do not change. To apply Eq. (3) more conveniently, we use the second method in the following.

4.1.1. Amplitude-damping channel

For an arbitrary operator

$$\boldsymbol{F} = \begin{pmatrix} F_{11} & F_{12} \\ F_{21} & F_{22} \end{pmatrix}, \tag{54}$$

the amplitude-damping channel is defined via the mapping

$$\varepsilon_{\rm A}^{\dagger}(\boldsymbol{F}) = \sum_{i=0}^{1} E_i^{\dagger} \boldsymbol{F} E_i \tag{55}$$

with

$$E_0 = \sqrt{s}|0\rangle\langle 0| + |1\rangle\langle 1|, \ E_1 = \sqrt{p}|1\rangle\langle 0|, \tag{56}$$

where E_0 and E_1 are the Kraus operators, $p = 1 - s$, $s = \exp[-\gamma t_0/2]$, and γ is the damping rate. According to the above mapping, we can obtain the three Pauli operators within this decoherence channel

$$\begin{aligned} &\varepsilon_{\rm A}^{\dagger}(\sigma_x) = \sqrt{s}\sigma_x, \quad \varepsilon_{\rm A}^{\dagger}(\sigma_y) = \sqrt{s}\sigma_y, \\ &\varepsilon_{\rm A}^{\dagger}(\sigma_z) = s\sigma_z - p. \end{aligned} \tag{57}$$

4.1.2. Phase-damping channel

In the phase-damping channel, the corresponding map is given by

$$\varepsilon_{\rm P}^{\dagger}(\boldsymbol{F}) = \sum_{i=0}^{2} E_i^{\dagger} \boldsymbol{F} E_i \tag{58}$$

with

$$\begin{aligned} &E_0 = \sqrt{s}\,\mathit{1}, \quad E_1 = \sqrt{p}|0\rangle\langle 0|, \\ &E_2 = \sqrt{p}|1\rangle\langle 1|, \end{aligned} \tag{59}$$

where $\mathit{1}$ is the identity operator. By a direct calculation, the three Pauli operators in this decoherence

channel are obtained as

$$\varepsilon_{\rm P}^{\dagger}(\sigma_x) = s\sigma_x, \quad \varepsilon_{\rm P}^{\dagger}(\sigma_y) = s\sigma_y,$$
$$\varepsilon_{\rm P}^{\dagger}(\sigma_z) = \sigma_z. \tag{60}$$

4.1.3. Depolarizing channel

Under this decoherence mechanism, the operator $\boldsymbol{F}$ is governed by the relation

$$\varepsilon_{\rm D}^{\dagger}(\boldsymbol{F}) = \sum_{i=0}^{3} E_i^{\dagger} \boldsymbol{F} E_i, \tag{61}$$

where four Kraus operators are defined as

$$E_0 = \sqrt{1 - \frac{3p}{4}}\, 1, \quad E_1 = \frac{p}{2}\sigma_x, \tag{62}$$
$$E_2 = \frac{p}{2}\sigma_y, \quad E_3 = \frac{p}{2}\sigma_z. \tag{63}$$

From the above mapping, we find

$$\varepsilon_{\rm D}^{\dagger}(\sigma_\alpha) = s\sigma_\alpha, \ \alpha \in \{x, y, z\}. \tag{64}$$

We consider the decoherence channels acting separately on each qubit of the system with three qubits, these expressions of operators for the single qubit are useful to obtain the expectation values of the collective operators with the decoherence.

4.2. Maximal and total skew information and concurrence

Now we study the maximal and the total skew information and the concurrence within the three different decoherence channels. From the previous analysis, the two kinds of information are determined by the expectation values of some collective operators. The expectation value of any observable $\varepsilon^{\dagger}(\boldsymbol{F})$ with decoherence within the Heisenberg picture can be obtained through

$$\langle \varepsilon^{\dagger}(\boldsymbol{F}) \rangle = {\rm Tr}[\varepsilon^{\dagger}(\boldsymbol{F})\rho], \tag{65}$$

where $\rho = |\psi(t)\rangle\langle\psi(t)|$, and $|\psi(t)\rangle$ can be obtained by the three models in Section 3. Considering the expressions of the two kinds of information and Eqs. (57), (60), and (64) for the different decoherence channels and using a straightforward calculation, we can obtain the MSI as

$$I_{\rm m,A} = \max(s^2 \Delta S_z^2,\ s \max \Delta S^2(x, y)), \tag{66}$$
$$I_{\rm m,P} = \max(\Delta S_z^2,\ s^2 \max \Delta S^2(x, y)), \tag{67}$$
$$I_{\rm m,D} = s^2 \max(\Delta S_z^2,\ \max \Delta S^2(x, y)). \tag{68}$$

From the definition of s, we have $s^2 < s$. Due to the fact that $\Delta S_z^2 < \max \Delta S^2(x, y)$ for state $\psi(t)$ in Section 3, in the ADC and the DPC the MSI is still in the (S_x, S_y) plane, then

$$I_{\rm m,A} = s \max \Delta S^2(x, y), \tag{69}$$
$$I_{\rm m,D} = s^2 \max \Delta S^2(x, y). \tag{70}$$

In the PDC, the decoherence does not affect the z-axis SI, then it is possible that the MSI turns to the z direction, so

$$I_{\rm m,P} = \max(\Delta S_z^2,\ s^2 \max \Delta S^2(x, y)). \tag{71}$$

Further, we can obtain the TSI in the three decoherence channels

$$I_{\rm sum,A} = s[S^2 + S - \langle S_z^2 \rangle] + s^2 \Delta S_z^2, \tag{72}$$
$$I_{\rm sum,P} = s^2(S^2 + S) + (1 - s^2)\langle S_z^2 \rangle - \langle S_z \rangle^2, \tag{73}$$
$$I_{\rm sum,D} = s^2 I_{\rm sum}. \tag{74}$$

In the above equations, $\langle S_z^2 \rangle$, $\langle S_z \rangle$, $\max \Delta S^2(x, y)$, and $I_{\rm sum}$ are given in Section 3. From Eqs. (69)–(74), we can see that due to the quantum decoherence, both the MSI and the TSI will gradually

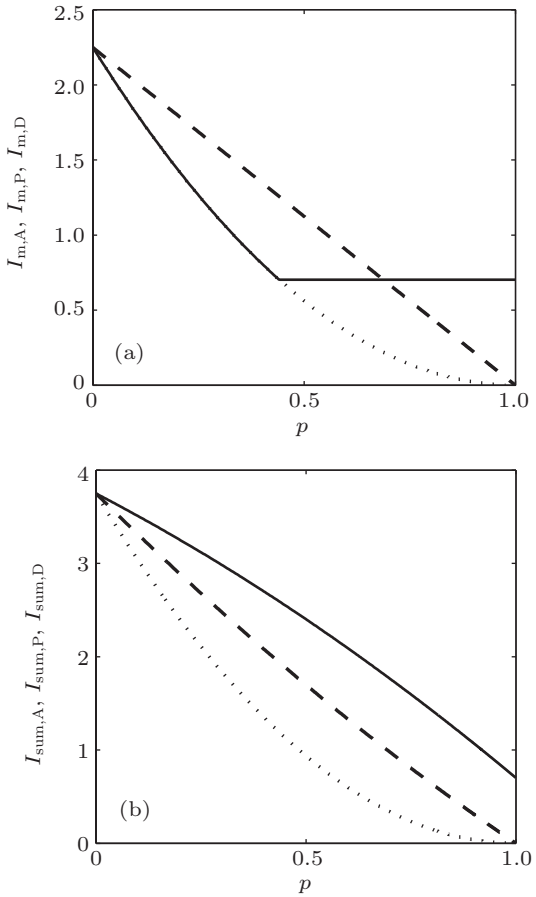


Fig. 4. (a) MSI and (b) TSI versus p in the three different decoherence channels. The three-qubit state is $|{\rm GHZ}\rangle_{S_y}$, and $\gamma = 1$. Dashed, solid, and dotted lines correspond the ADC, the PDC, and the DPC, respectively.

decrease. In the ADC and the DPC, they reach zero in the asymptotic limit of $s = 0$ regardless of their initial values, i.e., the information losses completely. In the PDC, if $\Delta S_z^2 \neq 0$, they do not loss completely in this limit and keep the z-axis SI. In Fig. 4, we present their evolutions in the different decoherence channels.

Through a simple calculation, we can see that the condition in which both the MSI and the TSI equal to zero is $s = 0$. In other words, the sudden death of the MSI and the TSI do not exist in any decoherence channel. However, the sudden death of the pairwise entanglement exists in these decoherence channels.[45] We can use the method in Ref. [45] to obtain the concurrence

$$C_{\rm A} = \max[0,\ s(C - px)], \tag{75}$$

$$C_{\rm P} = \max[0,\ s^2 C + (s^2 - 1)(1 - \langle\sigma_{1z}\sigma_{2z}\rangle)], \tag{76}$$

$$C_{\rm D} = \max[0,\ s^2 C + (s^2 - 1)], \tag{77}$$

where

$$C = \left|1 - \frac{2}{3}\left(\frac{15}{4} - \langle S_z^2\rangle + |\langle S_+^2\rangle|\right)\right| \Big/ 2, \tag{78}$$

$$x = 1 + 2\langle\sigma_{1z}\rangle + \langle\sigma_{1z}\sigma_{2z}\rangle, \tag{79}$$

$$\langle\sigma_{1z}\rangle = 2\langle S_z\rangle/3,\ \langle\sigma_{1z}\sigma_{2z}\rangle = 2\langle S_z^2\rangle/3 - 1/2. \tag{80}$$

As an example, in Fig. 5, plots of the concurrence of the state generated from $|111\rangle$ via the two-axis countertwisting model against p in the three different decoherence channels are shown. We observe the phenomenon of the sudden death of the pairwise entanglement. In the ADC, the entanglement capacity to overcome decoherence is more robust than that in the PDC and the DPC. In the same decoherence channel, different initial values of the concurrence correspond to different time of pairwise entanglement death.

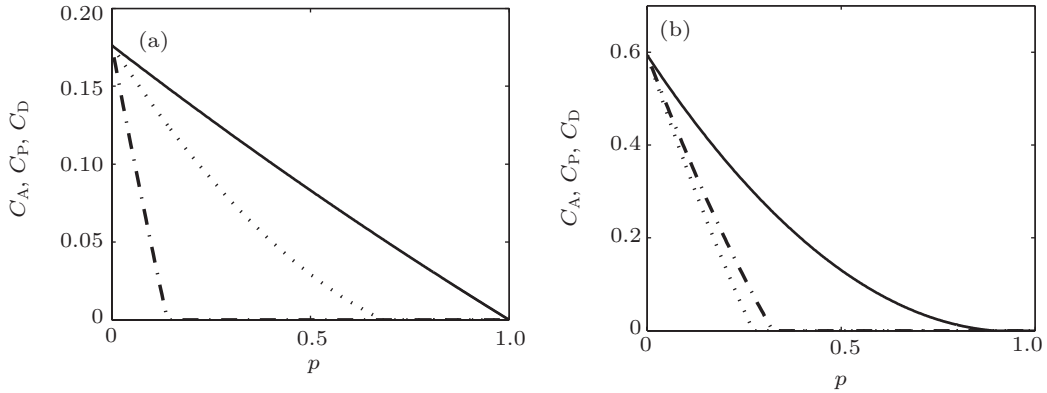


Fig. 5. Concurrence versus p in three different decoherent channels. In panels (a) and (b), the time of the state $\psi(t)$ is 0.1 and 0.3π, respectively, and $\gamma = 1$. Solid, dotted, and dot-dashed lines correspond the ADC, the PDC, and the DPC, respectively.

5. Conclusion

In conclusion, we have investigated the MSI and the TSI in three nonlinear models with three qubits. We present the state vectors at any time. Though the state vectors are different for different models, the MSI and the TSI have the same forms. There are no clear relations between them and concurrence C. We find that if condition $W \leq \chi/\sqrt{3}$ is satisfied, then the $|{\rm GHZ}\rangle_{S_y}$ state can occur, in which the MSI and the TSI synchronously reach the extreme values 15/4 and 9/4, respectively. For the models, the time of the occurrence of $|{\rm GHZ}\rangle_{S_y}$ is dependent on W, χ, and ΔE. Under the ADC and the DPC, both the MSI and the TSI completely loss, while under the PDC, the z-axis information is reserved. For the three decoherence channels, the phenomenon of the sudden death can be observed, but both the MSI and the TSI do not die suddenly.

References

[1] Kitagawa M and Ueda M 1993 *Phys. Rev.* A **47** 5138

[2] Wineland D J, Bollinger J J, Itano W M and Heinzen D J 1994 *Phys. Rev.* A **50** 67

[3] Yan D, Song L J and Chen D W 2009 *Acta Phys. Sin.* **58** 3679 (in Chinese)

[4] Wang X G and Sanders B C 2003 *Phys. Rev.* A **68** 012101

[5] Li Y, Castin Y and Sinatra A 2008 *Phys. Rev. Lett.* **100** 210401

[6] Li Y, Treutlein Y P, Reicheland J and Sinatra A 2009 *Eur. Phys. J.* B **68** 365

[7] Yang Y, Liu W F, Sun Z and Wang X G 2009 *Phys. Rev.* A **79** 054104

[8] Liu W F, Xiong H N, Ma J and Wang X G 2010 *Int. J. Theor. Phys.* **49** 1073

[9] Law C K, Ng H T and Leung P T 2001 *Phys. Rev.* A **63** 055601

[10] Jafarpour M and Akhound A 2007 *Phys. Lett.* A **372** 2374

[11] Sørensen A, Duan L M, Cirac I and Zoller P 2001 *Nature* **409** 63

[12] Poulsen U V and Molmer K 2001 *Phys. Rev.* A **64** 013616

[13] Helmerson K and You L 2001 *Phys. Rev. Lett.* **87** 170402

[14] Takeuchi M, Ichihara S, Takano T, Kumakura M, Yabuzaki T and Takahashi Y 2005 *Phys. Rev. Lett.* **94** 023003

[15] Jin G R and Kim S W 2007 *Phys. Rev.* A **76** 043621

[16] Jin G R and Kim S W 2007 *Phys. Rev. Lett.* **99** 170405

[17] Turchette Q A, Wood C S, King B E, Myatt C J, Leibfried D, Itano W M, Monroe C and Wineland D J 1998 *Phys. Rev. Lett.* **81** 3631

[18] Meyer V, Rowe M A, Kielpinski D, Sackett C A, Itano1 W M, Monroe C and Wineland D J 2001 *Phys. Rev. Lett.* **86** 5870

[19] Leibfried D, Barrett M D, Schaetz T, Britton J, Chiaverini J, Itano W M, Jost J D, Langer C and Wineland D J 2004 *Science* **304** 1476

[20] Hagley E, Maitre X, Nogues G, Wunderlich C, Brune M, Raimond J M and Haroche S 1997 *Phys. Rev. Lett.* **79** 1

[21] Messikh A, Ficek Z and Wahiddin M J 2003 *Phys. Rev.* A **68** 064301

[22] Zeng B, Zhou D L, Xu Z and You L 2005 *Phys. Rev.* A **71** 042317

[23] Wigner E P and Yanase M M 1963 *Proc. Natl. Acad. Sci.* US **49** 910

[24] Luo S L and Caves C M 1994 *Phys. Rev. Lett.* **72** 3439

[25] Wootters W K 1981 *Phys. Rev.* D **23** 357

[26] Luo S L 2000 *Lett. Math. Phys.* **53** 243

[27] Luo S L 2003 *Phys. Rev. Lett.* **91** 180403

[28] Luo S L 2003 *P. Am. Math. Soc.* **132** 885

[29] Chen Z Q 2005 *Phys. Rev.* A **71** 052302

[30] Gong L Y and Tong P Q 2008 *Chin. Phys.* B **17** 674

[31] W H F and Zhang S 2009 *Chin. Phys.* B **18** 2642

[32] Liu W C, Wang F Q and Liang R S 2010 *Chin. Phys.* B **19** 094204

[33] Li M, Fei S M and L J X Q 2010 *Chin. Phys.* B **19** 090315

[34] Connes A and Stormer E 1978 *J. Funct. Anal.* **28** 187

[35] Yan D, Wang X G and Wu L A 2005 *Chin. Phys. Lett.* **22** 521

[36] Yan D, Wang X G, Song L J and Zong Z G 2007 *Cent. Eur. J. Phys.* **5** 367

[37] Banacloche J G 1990 *Phys. Rev.* A **65** 3385

[38] Zurek W H, Habib S and Paz J P 1993 *Phys. Rev. Lett.* **70** 1187

[39] Raghavan S, Pu H and Bigelow N P 2010 *Opt. Commun.* **188** 149

[40] Milburn J, Corney J, Wright E M and Walls D F 1997 *Phys. Rev.* A **55** 4138

[41] Botet R, Jullien R and Pfeuty P 1982 *Phys. Rev. Lett.* **49** 478

[42] Cirac J, Lewenstein M, Mømer K and Zoller P 1998 *Phys. Rev.* A **57** 1208

[43] Garanin J, Hídalgo X M and Chudnovsky E M 1998 *Phys. Rev.* B **57** 13639

[44] Wang X G and Mømer K 2002 *Eur. Phys. J.* D **18** 385

[45] Wang X G, Miranowicz A, Liu Y X, Sun C P and Nori F 2010 *Phys. Rev.* A **81** 022106